

Stability of the Decoupled Extended Kalman Filter in the LSTM-Based Online Learning[☆]

N. Mert Vural^{a,*}, Suleyman S. Kozat^a

^a*Department of Electrical and Electronics Engineering, Bilkent University, Ankara, Turkey*

Abstract

We investigate the convergence and stability properties of the decoupled extended Kalman filter learning algorithm (DEKF) within the long-short term memory network (LSTM) based online learning framework. For this purpose, we model DEKF as a perturbed extended Kalman filter and derive sufficient conditions for its stability during the LSTM training. We show that if the perturbations -introduced due to decoupling- stay bounded, DEKF learns the LSTM parameters with similar convergence and stability properties of the global extended Kalman filter learning algorithm. We verify our results with several numerical simulations and compare DEKF with other LSTM training methods. In our simulations, we also observe that the well-known hyper-parameter selection approaches used for DEKF in the literature satisfy our conditions.

Keywords: Sequential learning, neural network training, Kalman filtering, long short term memory (LSTM), online learning, regression, stochastic gradient descent (SGD).

1. Introduction

Estimating an unknown desired signal is one of the main subjects of interest in the contemporary online learning literature [1]. In this problem, we sequentially receive a data sequence related to a desired signal to predict the signal's

[☆]This work is supported in part by TUBITAK Contract No. 117E153.

*Corresponding author

Email addresses: vural@ee.bilkent.edu.tr (N. Mert Vural), kozat@ee.bilkent.edu.tr (Suleyman S. Kozat)

next value [2]. This problem is also known as online regression, and it is extensively studied in the signal processing [3, 4, 5, 6], neural network [7, 8, 9, 10, 11], and machine learning literatures [1, 12, 13]. In these studies, nonlinear approaches are generally employed as linear modeling is inadequate for a wide range of applications due to the constraints on linearity [5, 14].

For the online regression task, there exists a wide range of nonlinear approaches in the machine learning and signal processing literatures [14, 15, 16]. However, most of these approaches usually suffer from high computational complexity, and they may provide poor performance due to stability and overfitting issues [5]. Neural network-based regression algorithms are also introduced for nonlinear modeling since neural networks are capable of modeling highly nonlinear and intricate structures [7, 11]. However, they are also shown to be prone to overfitting problems and demonstrate inadequate performance in certain applications [17]. To remedy these issues and further enhance their performance, neural networks composed of multiple layers, i.e., deep neural networks (DNNs), are recently introduced. In DNNs, a layered structure is employed so that each layer performs a feature extraction based on the previous layers [18]. With this mechanism, DNNs can model highly nonlinear and complex structures [18, 19]. However, this layered structure poorly performs in capturing time dependencies in the data [20]. Therefore, DNNs can provide only limited performance in modeling time series and processing temporal data [15, 20]. As a remedy, recurrent neural networks (RNNs) are used since these networks have internal memory that can store past information [15, 21]. However, basic RNNs lack control structures so that the long-term components cause either exponential growth or decay in the norm of gradients, which are the well-known exploding and vanishing gradient problems, respectively [22]. Therefore, they are insufficient to capture long-term dependencies on the data, which significantly restricts their performance in real-life tasks. In order to resolve this issue, a novel RNN architecture with several control structures, i.e., long-short term memory network (LSTM), is introduced [23]. In this study, we are particularly interested in nonlinear regression with the LSTM networks due to their superior perfor-

mance on capturing long-term dependencies. We note that the presented work in this paper can be generalized to the recurrent neural networks with smooth and bounded activation functions as well. However, since we utilize the LSTM structures due to our performance concern, in the rest of the paper, we present our work in an LSTM-oriented manner.

For the LSTM structures, there exist a wide range of online training methods to learn network parameters [15, 21, 24, 25, 26, 27]. Among them, the first-order gradient-based methods [21, 24] are widely preferred due to their efficiency. However, the first-order techniques, in general, provide poorer performance compared to the second-order techniques [26, 27], especially in the applications where the network parameters should be rapidly learned, e.g., when the data is scarce [28] or highly non-stationary [29]. As a second-order technique, the global extended Kalman filter (GEKF) learning algorithm has often been favored in terms of its accuracy and speed of convergence [30, 31]. On the other hand, the GEKF learning algorithm has cubic computational complexity in the parameter size of LSTM, which is usually prohibitive for the online regression task. To resolve this issue, the decoupled extended Kalman filter (DEKF) learning algorithm has been introduced in [32]. To reduce the computational requirement of GEKF, the DEKF learning algorithm ignores the interdependence of the mutually exclusive groups of the LSTM parameters, where the groups are determined by the user. Up to now, many studies empirically report that the DEKF learning algorithm provides comparable performance as GEKF with quadratic computational complexity in the parameter size [27, 32, 33, 34]. However, we emphasize that since DEKF has been considered as a heuristic to scale down GEKF in the neural network literature [15, 31], its convergence and stability properties have not been studied analytically. In this paper, we study the theoretical properties of the DEKF learning algorithm within the LSTM-based online regression framework.

In order to investigate the convergence and stability properties of DEKF, we model the effect of decoupling as perturbations introduced to GEKF during the LSTM training. We then extend the analysis in [35] for the LSTM-based online

regression case. Here, we show that if the perturbations due to decoupling stay bounded, DEKF learns the LSTM parameters with similar convergence and stability properties of GEKF by reducing its computational requirement to quadratic computational complexity in the parameter size. We verify our results with several numerical simulations and compare DEKF with other conventional LSTM training methods [15, 21, 24, 25, 27]. In our simulations, we also observe that the well-known hyper-parameter selection approaches used for DEKF in the literature [31, 32, 34] satisfy our conditions.

Our main contributions are as follows:

- To the best of our knowledge, we, as the first time in the neural network literature, study the DEKF learning algorithm analytically. We show that if the perturbations, which models the effect of decoupling, stay bounded, DEKF learns the LSTM parameters with similar convergence and stability properties of GEKF by reducing its computational requirement to quadratic computational complexity in the parameter size.
- In our simulations, we observe that the well-known hyper-parameter selection approaches used for DEKF in the literature [31, 32, 34] provide comparable performance with GEKF while satisfying our mathematically proven conditions. Therefore, we additionally provide theoretically founded experimental results, which can be used as a benchmark in future LSTM-based online learning studies.

This paper is organized as follows. In Section 2, we formally introduce the online regression problem and describe our LSTM model. In Section 3, we review the extended Kalman filter (EKF) based online LSTM training methods. Here, we compare their convergence properties and computational requirements to motivate the reader for the analysis in the following section. In Section 4, we derive the sufficient conditions for the stability of DEKF within the LSTM-based online regression framework. In Section 5, we verify our results with numerical simulations and compare DEKF with other LSTM training methods. We then finalize our paper with concluding remarks in Section 6.

2. Model and Problem Description

All vectors are column vectors and denoted by boldface lower case letters. Matrices are represented by boldface capital letters. The $\mathbf{0}$ represents a matrix or a vector of all zeros, whose dimensions are understood from the context. \mathbf{I} is the identity matrix, whose dimensions are understood from the context. $\|\cdot\|$ denotes the Euclidean norm of the vectors and the spectral norm of the matrices. $E[\mathbf{x}]$ is the expected value of \mathbf{x} , and $E[\mathbf{x}|\mathbf{y}]$ is the expected value of \mathbf{x} given \mathbf{y} . Given two matrices \mathbf{A} and \mathbf{B} , $\mathbf{A} > \mathbf{B}$ (respectively \geq) means that $(\mathbf{A} - \mathbf{B})$ is a positive definite (respectively semi-positive definite) matrix. Given two vectors \mathbf{x} and \mathbf{y} , $[\mathbf{x}; \mathbf{y}]$ is their vertical concatenation.

We define the online regression problem as follows: We sequentially receive $\{\mathbf{d}_t\}_{t \geq 1}$, $\mathbf{d}_t \in \mathbb{R}^{n_d}$, and input vectors, $\{\mathbf{x}_t\}_{t \geq 1}$, $\mathbf{x}_t \in \mathbb{R}^{n_i}$ such that our goal is to estimate \mathbf{d}_t based on our current and past observations $\{\cdots, \mathbf{x}_{t-1}, \mathbf{x}_t\}$. Given our estimate $\hat{\mathbf{d}}_t$, which can only be a function of $\{\cdots, \mathbf{x}_{t-1}, \mathbf{x}_t\}$ and $\{\cdots, \mathbf{d}_{t-2}, \mathbf{d}_{t-1}\}$, we suffer the loss $l(\mathbf{d}_t, \hat{\mathbf{d}}_t)$. The aim is to optimize the network with respect to the loss function $l(\cdot, \cdot)$. In this study, we particularly work with squared error, i.e., $l(\mathbf{d}_t, \hat{\mathbf{d}}_t) = \|\mathbf{d}_t - \hat{\mathbf{d}}_t\|^2$. However, our work can be extended for a wide range of cost functions (including the cross-entropy) using the analysis in [36, Section 3].

In this paper, we study online regression within the LSTM-based online learning framework. As illustrated in Fig. 1, we use the most widely used LSTM model, where the activation functions are set to the hyperbolic tangent function and the peep-hole connections are eliminated. As in Fig. 1, we use a single LSTM as the hidden layer and use an additional output layer, where the

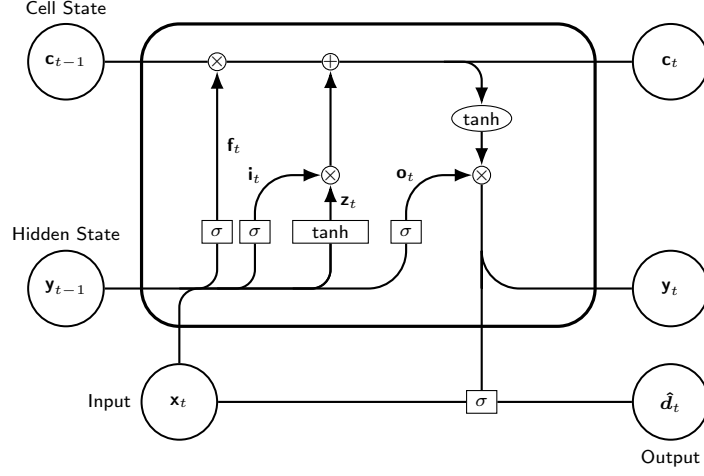


Figure 1: The detailed schematic of the equations given in (1)-(7).

activation function is chosen as the sigmoid function. Hence, we have:

$$\mathbf{z}_t = \tanh(\mathbf{W}^{(z)}[\mathbf{x}_t; \mathbf{y}_{t-1}]) \quad (1)$$

$$\mathbf{i}_t = \sigma(\mathbf{W}^{(i)}[\mathbf{x}_t; \mathbf{y}_{t-1}]) \quad (2)$$

$$\mathbf{f}_t = \sigma(\mathbf{W}^{(f)}[\mathbf{x}_t; \mathbf{y}_{t-1}]) \quad (3)$$

$$\mathbf{c}_t = \mathbf{i}_t \odot \mathbf{z}_t + \mathbf{f}_t \odot \mathbf{c}_{t-1} \quad (4)$$

$$\mathbf{o}_t = \sigma(\mathbf{W}^{(o)}[\mathbf{x}_t; \mathbf{y}_{t-1}]) \quad (5)$$

$$\mathbf{y}_t = \mathbf{o}_t \odot \tanh(\mathbf{c}_t) \quad (6)$$

$$\hat{\mathbf{d}}_t = \sigma(\mathbf{W}^{(d)}[\mathbf{x}_t; \mathbf{y}_t]) \quad (7)$$

where \odot denotes the element-wise multiplication, $\mathbf{c}_t \in \mathbb{R}^{n_s}$ is the state vector, $\mathbf{x}_t \in \mathbb{R}^{n_i}$ is the input vector, and $\mathbf{y}_t \in \mathbb{R}^{n_s}$ is the output vector and $\hat{\mathbf{d}}_t \in \mathbb{R}^{n_d}$ is our final estimation. Furthermore, \mathbf{i}_t , \mathbf{f}_t and \mathbf{o}_t are the input, forget and output gates respectively. The sigmoid function $\sigma(\cdot)$ and the hyperbolic tangent function $\tanh(\cdot)$ applies point wise to the vector elements. The weight matrices are $\mathbf{W}^{(z)}$, $\mathbf{W}^{(i)}$, $\mathbf{W}^{(f)}$, $\mathbf{W}^{(o)} \in \mathbb{R}^{n_s \times (n_i + n_s)}$ and $\mathbf{W}^{(d)} \in \mathbb{R}^{n_d \times (n_i + n_s)}$. We note that although we do not explicitly write the bias terms, they can be included in (1)-(7) by augmenting the input vector with a constant dimension.

3. EKF-Based Online Training Algorithms

In this section, we demonstrate the EKF-based online training algorithms to learn the LSTM parameters for the online regression task. We note that the aim of this section is to compare the convergence properties and the computational requirements of the demonstrated algorithms to motivate the reader for our analysis in the next section. In the following, we present the global EKF [31], independent EKF [37], and decoupled EKF [32] learning algorithms, respectively.

3.1. Online Learning with the Global EKF Learning Algorithm

In order to convert the LSTM training into a filtering problem, we model the desired signal as an autoregressive process, which is realized by the LSTM network in (1)-(7). For notational convenience, we group all the LSTM parameters, i.e., $\mathbf{W}^{(z)}, \mathbf{W}^{(i)}, \mathbf{W}^{(f)}, \mathbf{W}^{(o)} \in \mathbb{R}^{n_s \times (n_i + n_s)}$ and $\mathbf{W}^{(d)} \in \mathbb{R}^{n_d \times (n_i + n_s)}$, into a vector $\boldsymbol{\theta}_t \in \mathbb{R}^{n_\theta}$, where $n_\theta = (4n_s + n_d)(n_s + n_i)$. We then describe the underlying process of the incoming data stream with a state-space model:

$$\begin{bmatrix} \boldsymbol{\theta}_t \\ \mathbf{c}_t \\ \mathbf{y}_t \end{bmatrix} = \begin{bmatrix} \boldsymbol{\theta}_{t-1} \\ f(\mathbf{y}_{t-1}, \mathbf{c}_{t-1}, \mathbf{x}_t; \boldsymbol{\theta}_t) \\ g(\mathbf{y}_{t-1}, \mathbf{c}_t, \mathbf{x}_t; \boldsymbol{\theta}_t) \end{bmatrix} + \begin{bmatrix} \mathbf{q}_t \\ \mathbf{0} \\ \mathbf{0} \end{bmatrix} \quad (8)$$

$$\mathbf{d}_t = h(\mathbf{y}_t, \mathbf{x}_t; \boldsymbol{\theta}_t) + \mathbf{v}_t. \quad (9)$$

Here, we represent the optimal LSTM parameters that realize the incoming data stream with a vector $\boldsymbol{\theta}_t \in \mathbb{R}^{n_\theta}$, which is modeled as a stationary process. We use $f(\cdot; \boldsymbol{\theta}_t)$ and $g(\cdot; \boldsymbol{\theta}_t)$ in (8) to represent equations in (1)-(4) and (5)-(6) parametrized by $\boldsymbol{\theta}_t$. We use $h(\cdot; \boldsymbol{\theta}_t)$ in (9) to represent (7) parametrized by $\boldsymbol{\theta}_t$. The process noise $\mathbf{q}_t \in \mathbb{R}^{n_\theta}$ and the measurement noise $\mathbf{v}_t \in \mathbb{R}^{n_d}$ are the artificial noise terms, which are used to enhance the training performance [15, 33]. The noise components are assumed to be Gaussian, i.e., $\mathbf{q}_t \sim \mathcal{N}(\mathbf{0}, \mathbf{Q}_t)$ and $\mathbf{v}_t \sim \mathcal{N}(\mathbf{0}, \mathbf{R}_t)$. In order to efficiently implement the training algorithms, we use diagonal matrices for the covariance matrices of the artificial noise terms, i.e., $\mathbf{Q}_t = q_t \mathbf{I}$ and $\mathbf{R}_t = r_t \mathbf{I}$, where $q_t, r_t > 0$.

The global EKF (GEKF) learning algorithm is the EKF applied to the state-space model in (8)-(9) to estimate the network parameters $\boldsymbol{\theta}_t$ [31]. In the algorithm, we first perform the forward LSTM-propagation with (1)-(7) by using the parameters $\hat{\boldsymbol{\theta}}_t \in \mathbb{R}^{n_\theta}$, which is our estimate for the optimum weights at time step t . Then, we perform the weight updates with the following formulas:

$$\hat{\boldsymbol{\theta}}_{t+1} = \hat{\boldsymbol{\theta}}_t + \mathbf{K}_t(\mathbf{d}_t - \hat{\mathbf{d}}_t) \quad (10)$$

$$\mathbf{P}_{t+1} = (\mathbf{I} - \mathbf{K}_t \mathbf{H}_t) \mathbf{P}_t + \mathbf{Q}_t \quad (11)$$

$$\mathbf{H}_t = \left. \frac{\partial h(\mathbf{y}_t, \mathbf{x}_t; \boldsymbol{\theta})}{\partial \boldsymbol{\theta}} \right|_{\boldsymbol{\theta}=\hat{\boldsymbol{\theta}}_t} \quad (12)$$

$$\mathbf{K}_t = \mathbf{P}_t \mathbf{H}_t^T (\mathbf{H}_t \mathbf{P}_t \mathbf{H}_t^T + \mathbf{R}_t)^{-1}. \quad (13)$$

Here, $\mathbf{P}_t \in \mathbb{R}^{n_\theta \times n_\theta}$ is the state covariance matrix, which models the interactions between each pair of the LSTM parameters, $\mathbf{K}_t \in \mathbb{R}^{n_\theta \times n_d}$ is the Kalman gain matrix, and $\mathbf{H}_t \in \mathbb{R}^{n_d \times n_\theta}$ is the Jacobian matrix of $h(\cdot; \boldsymbol{\theta}_t)$ evaluated at $\hat{\boldsymbol{\theta}}_t$. The derivations for the Jacobian matrix \mathbf{H}_t are given in Appendix A. We note that due to (11), the computational complexity of the GEKF learning algorithm is $O(n_\theta^3)$, which is usually a prohibitive computational requirement for the online settings.¹

3.2. Online Learning with the Independent EKF Learning Algorithm

To reduce the complexity of GEKF and make the training scalable, the independent EKF (IEKF) learning algorithm has been introduced in [37]. Here, the LSTM parameters are partitioned into g mutually exclusive groups, and each group is assumed independent.² Therefore, the weight updates are performed

¹We use big- O notation, i.e., $O(f(x))$, to ignore constant factors.

²For notational simplicity, we assume that each group contains the same number of weights. However, we note that IEKF allows partitioning the weights in an unbalanced manner as well.

as

$$\text{for } i = 1, \dots, g \quad (14)$$

$$\hat{\boldsymbol{\theta}}_{i,t+1} = \hat{\boldsymbol{\theta}}_{i,t} + \mathbf{K}_{i,t}(\mathbf{d}_t - \hat{\mathbf{d}}_t) \quad (15)$$

$$\mathbf{P}_{i,t+1} = (\mathbf{I} - \mathbf{K}_{i,t}\mathbf{H}_{i,t})\mathbf{P}_{i,t} + \mathbf{Q}_{i,t} \quad (16)$$

$$\mathbf{H}_{i,t} = \left. \frac{\partial h(\mathbf{y}_t, \mathbf{x}_t; \boldsymbol{\theta})}{\partial \boldsymbol{\theta}_i} \right|_{\boldsymbol{\theta}_i = \hat{\boldsymbol{\theta}}_{i,t}} \quad (17)$$

$$\mathbf{K}_{i,t} = \mathbf{P}_{i,t}\mathbf{H}_{i,t}^T(\mathbf{H}_{i,t}\mathbf{P}_{i,t}\mathbf{H}_{i,t}^T + \mathbf{R}_t)^{-1}, \quad (18)$$

where $\mathbf{P}_{i,t} \in \mathbb{R}^{\frac{n_\theta}{g} \times \frac{n_\theta}{g}}$ is the state covariance matrix, $\mathbf{H}_{i,t} \in \mathbb{R}^{n_d \times \frac{n_\theta}{g}}$ is the Jacobian matrix of $h(\cdot; \boldsymbol{\theta}_t)$ and $\mathbf{K}_{i,t} \in \mathbb{R}^{\frac{n_\theta}{g} \times n_d}$ is the Kalman gain matrix corresponding to the LSTM parameters in group i . Here, since we perform (16) g times, the computational complexity of the IEKF learning algorithm is $O(n_\theta^3/g^2)$, which can be significantly less than the computational complexity of GEKF. However, assuming each group is entirely independent may result in poor performance and requires a better initialization for the stability [31, 34].

3.3. Online Learning with the Decoupled EKF Learning Algorithm

As an alternative solution to reduce the complexity of GEKF, the decoupled EKF (DEKF) learning algorithm has been introduced in [32] and successfully applied in the training of the RNN and LSTM structures [15, 32, 27, 25]. In DEKF, we again partition the LSTM parameters into g mutually exclusive groups; however, unlike IEKF, the groups are updated in an interdependent way. This is done by changing the Kalman gain formula in (18) as

$$\mathbf{K}_{i,t} = \mathbf{P}_{i,t}\mathbf{H}_{i,t}^T \left(\sum_{i=1}^g \mathbf{H}_{i,t}\mathbf{P}_{i,t}\mathbf{H}_{i,t}^T + \mathbf{R}_t \right)^{-1}. \quad (19)$$

Since the summation term in (19) can be computed only one time at the beginning of each time step, the Kalman gain formulation of DEKF does not increase the computational complexity. Therefore, the complexity of the DEKF learning algorithm is also $O(n_\theta^3/g^2)$.

Remark 3.1. By using the analysis in [35], we can derive sufficient conditions for the stability of the GEKF learning algorithm within the LSTM-based online

$$\mathbf{D}_i = \begin{matrix} & \begin{matrix} \overbrace{1} & \cdots & \overbrace{i} & \cdots & \overbrace{g} \end{matrix} \\ \begin{matrix} 1 \{ \\ \vdots \{ \\ i \{ \\ \vdots \{ \\ g \{ \end{matrix} & \left[\begin{array}{ccccc} \mathbf{0} & & \mathbf{0} & & \mathbf{0} \\ & \ddots & & \ddots & \\ \mathbf{0} & & \mathbf{I} & & \mathbf{0} \\ & \ddots & & \ddots & \\ \mathbf{0} & & \mathbf{0} & & \mathbf{0} \end{array} \right] \end{matrix} \end{matrix} \quad n_g \times n_g$$

Figure 2: The figure representation of the matrix \mathbf{D}_i .

learning framework. By following the same derivations and representing the effect of independent groups as non-linearity, we can derive sufficient conditions for the stability of the IEKF learning algorithm as well. However, since the convergence rate and the initialization performance of the EKF-based training algorithms are inversely proportional to the effect of the non-linearity [35], the IEKF learning algorithm converges slower and requires a better initialization than GEKF [31, 34]. On the other hand, although the DEKF learning algorithm is reported to provide comparable performance as GEKF with the same computational complexity of IEKF [15, 25, 27, 32], to the best of our knowledge, the stability of the DEKF learning algorithm is not analytically investigated in the neural network literature. In the next section, we derive sufficient conditions for the stability of the DEKF learning algorithm used in the online LSTM training. To this end, we model the effect of decoupling as perturbations introduced to GEKF during the LSTM training, and extend the conditions in [35] for the LSTM-based online regression case. We additionally show that if the perturbations introduced due to decoupling stay bounded, DEKF learns the LSTM parameters with similar theoretical properties of the GEKF learning algorithm by reducing its computational requirement to quadratic computational complexity in the parameter size.

4. Stability Analysis of the DEKF Learning Algorithm

In this section, we derive sufficient conditions for the stability of the DEKF learning algorithm within the LSTM-based online regression framework. We first rewrite the DEKF equations in (15)-(17) and (19) similar to the equations of GEKF in (10)-(13) by introducing perturbation:

$$\hat{\boldsymbol{\theta}}_{t+1} = \hat{\boldsymbol{\theta}}_t + \mathbf{K}_t(\mathbf{d}_t - \hat{\mathbf{d}}_t) \quad (20)$$

$$\tilde{\mathbf{P}}_{t+1} = (\mathbf{I} - \mathbf{K}_t \mathbf{H}_t) \mathbf{P}_t \quad (21)$$

$$\mathbf{P}_{t+1} = \sum_{i=1}^g \mathbf{D}_i \tilde{\mathbf{P}}_{t+1} \mathbf{D}_i + \mathbf{Q}_t \quad (22)$$

$$\mathbf{H}_t = \left. \frac{\partial h_t(\{\mathbf{x}\}_{t \geq 1}; \boldsymbol{\theta})}{\partial \boldsymbol{\theta}} \right|_{\boldsymbol{\theta} = \hat{\boldsymbol{\theta}}_t} \quad (23)$$

$$\mathbf{K}_t = \mathbf{P}_t \mathbf{H}_t^T (\mathbf{H}_t \mathbf{P}_t \mathbf{H}_t^T + \mathbf{R}_t)^{-1}. \quad (24)$$

Here, the update step from \mathbf{P}_t to $\tilde{\mathbf{P}}_{t+1}$ in (21) is formulated as in the update rule of the GEKF learning algorithm in (11). The state covariance matrix of the DEKF learning algorithm, i.e. \mathbf{P}_{t+1} , is formulated as a perturbed version of $\tilde{\mathbf{P}}_{t+1}$, where we introduce the perturbation through the matrices $\mathbf{D}_i \in \mathbb{R}^{n_\theta \times n_\theta}$, $i \in \{1, \dots, g\}$. As shown in Fig. 2, \mathbf{D}_i is an $n_\theta \times n_\theta$ matrix, whose i^{th} diagonal block is \mathbf{I} and all of the other entries are 0. By (21)-(22), we equivalently write (19) as the perturbed covariance matrix update of GEKF defined in (11).

In order to write the error dynamics of DEKF, we write the Taylor expansion of $h(\mathbf{y}_t, \mathbf{x}_t; \boldsymbol{\theta}_t)$ around $\hat{\boldsymbol{\theta}}_t$ as

$$h(\mathbf{y}_t, \mathbf{x}_t; \boldsymbol{\theta}_t) = h(\mathbf{y}_t, \mathbf{x}_t; \hat{\boldsymbol{\theta}}_t) + \mathbf{H}_t(\boldsymbol{\theta}_t - \hat{\boldsymbol{\theta}}_t) + \chi_t(\boldsymbol{\theta}_t, \hat{\boldsymbol{\theta}}_t) \quad (25)$$

where $\chi_t(\boldsymbol{\theta}_t, \hat{\boldsymbol{\theta}}_t)$ stands for the non-linear terms in the expansion. We note that in (25), $h(\mathbf{y}_t, \mathbf{x}_t; \boldsymbol{\theta}_t) = \mathbf{d}_t$ and $h(\mathbf{y}_t, \mathbf{x}_t; \hat{\boldsymbol{\theta}}_t) = \hat{\mathbf{d}}_t$. Let us say \mathbf{e}_t is the error between the optimum and the estimated network parameters at round t , i.e.,

$\mathbf{e}_t = \boldsymbol{\theta}_t - \hat{\boldsymbol{\theta}}_t$. By using (20)-(24), the error dynamics of DEKF are given as

$$\mathbf{e}_{t+1} = (\mathbf{I} - \mathbf{K}_t \mathbf{H}_t) \mathbf{e}_t + \mathbf{r}_t + \mathbf{s}_t \quad (26)$$

$$\mathbf{r}_t = -\mathbf{K}_t \chi_t(\boldsymbol{\theta}_t, \hat{\boldsymbol{\theta}}_t) \quad (27)$$

$$\mathbf{s}_t = \mathbf{q}_t - \mathbf{K}_t \mathbf{v}_t. \quad (28)$$

In the following theorem, we provide sufficient conditions for the stability of DEKF in the LSTM-based online regression task.

Theorem 4.1. *Consider the LSTM network described by the equations in (1)-(7) trained with the DEKF learning algorithm defined by (20)-(24). The DEKF learning algorithm asymptotically converges to the local optimum with probability one, if the following conditions hold:*

1. *There are positive real numbers $\underline{r}, \underline{p}, \bar{p} > 0$ such that the following bounds hold for every $t \geq 0$:*

$$\underline{p} \mathbf{I} \leq \mathbf{P}_t \leq \bar{p} \mathbf{I} \quad (29)$$

$$\underline{r} \mathbf{I} \leq \mathbf{R}_t. \quad (30)$$

2. *The process noise matrix \mathbf{Q}_t is lower bounded by*

$$(\tilde{\lambda}_t + \underline{q}) \mathbf{I} \leq \mathbf{Q}_t, \quad (31)$$

where \underline{q} is a positive number, i.e., $\underline{q} > 0$, and

$$\tilde{\lambda}_t = \max_{j \in \{1, \dots, n_\theta\}} |\lambda_j(\tilde{\mathbf{A}}_t) - \lambda_j(\mathbf{A}_t)|, \quad (32)$$

where

$$\begin{aligned} \mathbf{A}_t &= (\mathbf{I} - \mathbf{K}_t \mathbf{H}_t) \mathbf{P}_t (\mathbf{I} - \mathbf{K}_t \mathbf{H}_t)^T \\ \tilde{\mathbf{A}}_t &= \sum_{i=1}^g \mathbf{D}_i (\mathbf{I} - \mathbf{K}_t \mathbf{H}_t) \mathbf{P}_t (\mathbf{I} - \mathbf{K}_t \mathbf{H}_t)^T \mathbf{D}_i, \end{aligned}$$

and $\lambda_j(\mathbf{A}_t)$, $\lambda_j(\tilde{\mathbf{A}}_t)$ represent their j^{th} eigenvalues.

3. The initial error, i.e., $\mathbf{e}_0 = \boldsymbol{\theta}_0 - \hat{\boldsymbol{\theta}}_0$, and the covariance matrices of the artificial noise terms are upper bounded by

$$\|\mathbf{e}_0\| \leq \epsilon \quad (33)$$

$$\mathbf{Q}_t \leq \delta \mathbf{I} \quad (34)$$

$$\mathbf{R}_t \leq \delta \mathbf{I} \quad (35)$$

for some $\delta, \epsilon > 0$.

Remark 4.1. In the DEKF learning algorithm, the user determines the covariance matrices of the artificial noise terms \mathbf{Q}_t and \mathbf{R}_t , i.e., the conditions in (30), (31), (34), and (35) can be satisfied by the user. Therefore, Theorem 4.1 should be understood as a test mechanism, where (29) can be verified during training. If the numerically calculated values for \mathbf{P}_t is bounded, then the resulting weights are reliable in the sense of Theorem 4.1.

Remark 4.2. The following proof for Theorem 4.1 yields us explicit estimation formulas for ϵ and δ in (33) and (34)-(35). However, these estimates are generally very conservative as discussed in [35, Section V]. Therefore, in the following, we assume that as long as the covariance matrices of the artificial noise terms stay bounded, they satisfy (34)-(35). Moreover, we assume the conventional weight initialization methods utilized in the literature [23, 25, 27] are sufficient to satisfy (33).

In the following lemma, we provide two inequalities for the proof of Theorem 4.1 by using the properties of the LSTM model in (1)-(7).

Lemma 4.2. The considered LSTM model (1)-(7) guarantees two properties:

1. The Jacobian matrix \mathbf{H}_t in (23) is bounded as such there exists a positive real number \bar{h} that satisfies

$$\|\mathbf{H}_t\| \leq \bar{h} \quad (36)$$

for every $t \geq 0$.

2. The non-linearity term $\chi_t(\cdot, \cdot)$ in (25) is bounded as such there exist positive real numbers $\epsilon_\chi, \kappa_\chi > 0$ that satisfy

$$\|\chi_t(\boldsymbol{\theta}_t, \hat{\boldsymbol{\theta}}_t)\| \leq \kappa_\chi \|\boldsymbol{\theta}_t - \hat{\boldsymbol{\theta}}_t\| \quad (37)$$

with $\|\boldsymbol{\theta}_t - \hat{\boldsymbol{\theta}}_t\| \leq \epsilon_\chi$ for every $t \geq 0$.

Proof. 1. We note that for any $\mathbf{x}_t, \mathbf{y}_{t-1}$, and \mathbf{c}_{t-1} , the LSTM model in (1)-(7) is continuous with respect to the network parameters. Since the composite continuous mappings are continuous [38, Proposition 8.4], any recursive function based on our LSTM model is also continuous, which leads to the statement in (36).

2. Let us rewrite the Taylor expansion in (25) as

$$\chi_t(\boldsymbol{\theta}_t, \hat{\boldsymbol{\theta}}_t) = \hat{\mathbf{d}}_t - \mathbf{d}_t - \mathbf{H}_t(\boldsymbol{\theta}_t - \hat{\boldsymbol{\theta}}_t). \quad (38)$$

We note that $\hat{\mathbf{d}}_t, \mathbf{d}_t \in [0, 1]^{n_d}$, and that \mathbf{H}_t is bounded. Therefore, $\chi_t(\boldsymbol{\theta}_t, \hat{\boldsymbol{\theta}}_t)$ is also bounded and guarantees the statement in (37). \square

We utilize three additional lemmas for the proof:

Lemma 4.3. *Under the conditions of Theorem 4.1, if we choose*

$$(\tilde{\lambda}_t + \underline{q})\mathbf{I} \leq \mathbf{Q}_t, \quad (39)$$

where $\tilde{\lambda}_t$ is defined in (32), then

$$(\mathbf{I} - \mathbf{K}_t \mathbf{H}_t)^T \mathbf{P}_{t+1}^{-1} (\mathbf{I} - \mathbf{K}_t \mathbf{H}_t) \leq (1 - \alpha) \mathbf{P}_t^{-1} \quad (40)$$

where $(1 - \alpha) = \left[1 + \frac{q}{\bar{p}(1 + \frac{\bar{p}h}{\underline{c}})^2}\right]^{-1}$, $t > 0$.

Proof. We first write equations in (21) and (22) together as

$$\mathbf{P}_{t+1} = \sum_{i=1}^g \mathbf{D}_i (\mathbf{I} - \mathbf{K}_t \mathbf{H}_t) \mathbf{P}_t (\mathbf{I} - \mathbf{K}_t \mathbf{H}_t)^T \mathbf{D}_i + \mathbf{Q}_t \quad (41)$$

$$+ \sum_{i=1}^g \mathbf{D}_i \mathbf{K}_t \mathbf{H}_t \mathbf{P}_t (\mathbf{I} - \mathbf{K}_t \mathbf{H}_t)^T \mathbf{D}_i. \quad (42)$$

In the first step of the proof, we show that

$$\sum_{i=1}^g \mathbf{D}_i \mathbf{K}_t \mathbf{H}_t \mathbf{P}_t (\mathbf{I} - \mathbf{K}_t \mathbf{H}_t)^T \mathbf{D}_i \geq 0. \quad (43)$$

For this, it is sufficient to show

$$\mathbf{K}_t \mathbf{H}_t \mathbf{P}_t (\mathbf{I} - \mathbf{K}_t \mathbf{H}_t)^T = \mathbf{K}_t \mathbf{H}_t [(\mathbf{I} - \mathbf{K}_t \mathbf{H}_t) \mathbf{P}_t]^T \geq 0. \quad (44)$$

By using (24), (29) and (36), we obtain

$$\mathbf{K}_t \mathbf{H}_t = \mathbf{P}_t \mathbf{H}_t^T (\mathbf{H}_t \mathbf{P}_t \mathbf{H}_t^T + \mathbf{R}_t)^{-1} \mathbf{H}_t \geq 0. \quad (45)$$

By using (24), we write

$$(\mathbf{I} - \mathbf{K}_t \mathbf{H}_t) \mathbf{P}_t = \mathbf{P}_t - \mathbf{P}_t \mathbf{H}_t^T (\mathbf{H}_t \mathbf{P}_t \mathbf{H}_t^T + \mathbf{R}_t)^{-1} \mathbf{H}_t \mathbf{P}_t. \quad (46)$$

Applying the matrix inversion lemma,

$$[(\mathbf{I} - \mathbf{K}_t \mathbf{H}_t) \mathbf{P}_t]^{-1} = \mathbf{P}_t^{-1} + \mathbf{H}_t \mathbf{R}_t^{-1} \mathbf{H}_t > 0 \quad (47)$$

which proves (44), therefore (43). Then, we write

$$\mathbf{P}_{t+1} \geq \sum_{i=1}^g \mathbf{D}_i (\mathbf{I} - \mathbf{K}_t \mathbf{H}_t) \mathbf{P}_t (\mathbf{I} - \mathbf{K}_t \mathbf{H}_t)^T \mathbf{D}_i + \mathbf{Q}_t. \quad (48)$$

By selecting

$$(\tilde{\lambda}_t + \underline{q}) \mathbf{I} \leq \mathbf{Q}_t \quad (49)$$

we write

$$\begin{aligned} \mathbf{P}_{t+1} &\geq (\mathbf{I} - \mathbf{K}_t \mathbf{H}_t) \mathbf{P}_t (\mathbf{I} - \mathbf{K}_t \mathbf{H}_t)^T + \underline{q} \mathbf{I} \\ &= (\mathbf{I} - \mathbf{K}_t \mathbf{H}_t) [\mathbf{P}_t + \underline{q} (\mathbf{I} - \mathbf{K}_t \mathbf{H}_t)^{-1} (\mathbf{I} - \mathbf{K}_t \mathbf{H}_t)^{-T}] \\ &\quad \times (\mathbf{I} - \mathbf{K}_t \mathbf{H}_t)^T. \end{aligned} \quad (50)$$

Here, we note that (47) implies that $(\mathbf{I} - \mathbf{K}_t \mathbf{H}_t)^{-1}$ exists. Then, we take the

inverse of both sides of (50) and obtain

$$\begin{aligned}
(\mathbf{I} - \mathbf{K}_t \mathbf{H}_t)^T \mathbf{P}_{t+1}^{-1} (\mathbf{I} - \mathbf{K}_t \mathbf{H}_t) &\leq [\mathbf{P}_t + \underline{q}(\mathbf{I} - \mathbf{K}_t \mathbf{H}_t)^{-1}(\mathbf{I} - \mathbf{K}_t \mathbf{H}_t)^{-T}]^{-1} \\
&\leq \left[\mathbf{P}_t + \frac{\underline{q}}{(1 + \frac{\bar{p}\bar{h}}{\underline{r}})^2} \mathbf{I} \right]^{-1} \tag{51}
\end{aligned}$$

$$\leq \left[1 + \frac{\underline{q}}{\bar{p}(1 + \frac{\bar{p}\bar{h}}{\underline{r}})^2} \right]^{-1} \mathbf{P}_t^{-1} \tag{52}$$

$$= (1 - \alpha) \mathbf{P}_t^{-1} \tag{53}$$

where we use (29) and (36) for (51)-(52), and say $(1 - \alpha) = \left[1 + \frac{\underline{q}}{\bar{p}(1 + \frac{\bar{p}\bar{h}}{\underline{r}})^2} \right]^{-1}$. \square

Lemma 4.4. *Under the conditions of Theorem 4.1, there exists a positive scalar $\kappa_{\text{nonl}} > 0$ such that*

$$\mathbf{r}_t^T \mathbf{P}_{t+1}^{-1} [2(\mathbf{I} - \mathbf{K}_t \mathbf{H}_t)(\boldsymbol{\theta}_t - \hat{\boldsymbol{\theta}}_t) + \mathbf{r}_t] \leq \kappa_{\text{nonl}} \|\boldsymbol{\theta}_t - \hat{\boldsymbol{\theta}}_t\|^3 \tag{54}$$

holds for $\|\boldsymbol{\theta}_t - \hat{\boldsymbol{\theta}}_t\| \leq \epsilon_\chi$.

Proof. By using (24), (30) and (36), we write

$$\|\mathbf{K}_t\| \leq \frac{\bar{p}\bar{h}}{\underline{r}}. \tag{55}$$

Using this bound in (27), we write

$$\|\mathbf{r}_t\| \leq \frac{\bar{p}\bar{h}}{\underline{r}} \|\chi_t(\{\mathbf{x}\}_{t \geq 1}, \boldsymbol{\theta}_t, \hat{\boldsymbol{\theta}}_t)\|. \tag{56}$$

By (37), we write

$$\|\mathbf{r}_t\| \leq \frac{\bar{p}\bar{h}}{\underline{r}} \kappa_\chi \|\boldsymbol{\theta}_t - \hat{\boldsymbol{\theta}}_t\|^2 \tag{57}$$

for $\|\boldsymbol{\theta}_t - \hat{\boldsymbol{\theta}}_t\| \leq \epsilon_\chi$. Say $\kappa' = \frac{\bar{p}\bar{h}}{\underline{r}} \kappa_\chi$. Then

$$\begin{aligned}
&\mathbf{r}_t^T \mathbf{P}_{t+1}^{-1} [2(\mathbf{I} - \mathbf{K}_t \mathbf{H}_t)(\boldsymbol{\theta}_t - \hat{\boldsymbol{\theta}}_t) + \mathbf{r}_t] \\
&\leq \frac{\kappa'}{\underline{p}} \|\boldsymbol{\theta}_t - \hat{\boldsymbol{\theta}}_t\|^2 [2(1 + \frac{\bar{p}\bar{h}}{\underline{r}}) \|\boldsymbol{\theta}_t - \hat{\boldsymbol{\theta}}_t\| + \kappa' \epsilon_\chi \|\boldsymbol{\theta}_t - \hat{\boldsymbol{\theta}}_t\|] \\
&= \frac{\kappa'}{\underline{p}} [2(1 + \frac{\bar{p}\bar{h}}{\underline{r}}) + \kappa' \epsilon_\chi] \|\boldsymbol{\theta}_t - \hat{\boldsymbol{\theta}}_t\|^3 \\
&= \kappa_{\text{nonl}} \|\boldsymbol{\theta}_t - \hat{\boldsymbol{\theta}}_t\|^3.
\end{aligned}$$

□

Lemma 4.5. *Under the conditions of Theorem 4.1, there exists a positive scalar $\kappa_{noise} > 0$ independent of δ , such that*

$$E[\mathbf{s}_t^T \mathbf{P}_{t+1}^{-1} \mathbf{s}_t] \leq \kappa_{noise} \delta \quad (58)$$

holds for all $t > 0$.

Proof. By using (28)

$$\begin{aligned} E[\mathbf{s}_t^T \mathbf{P}_{t+1}^{-1} \mathbf{s}_t] &= E[(\mathbf{q}_t - \mathbf{K}_t \mathbf{v}_t)^T \mathbf{P}_{t+1}^{-1} (\mathbf{q}_t - \mathbf{K}_t \mathbf{v}_t)] \\ &= E[\mathbf{q}_t^T \mathbf{P}_{t+1}^{-1} \mathbf{q}_t] + E[\mathbf{v}_t^T \mathbf{K}_t^T \mathbf{P}_{t+1}^{-1} \mathbf{K}_t \mathbf{v}_t] \\ &\leq \frac{E[\mathbf{q}_t^T \mathbf{q}_t]}{\underline{p}} + \left(\frac{\bar{p}\bar{h}}{\underline{r}}\right)^2 \frac{E[\mathbf{v}_t^T \mathbf{v}_t]}{\underline{p}} \\ &\leq \frac{q\delta}{\underline{p}} + \left(\frac{\bar{p}\bar{h}}{\underline{r}}\right)^2 \frac{m\delta}{\underline{p}} \\ &= \kappa_{noise} \delta \end{aligned} \quad (59)$$

where $\kappa_{noise} = \frac{q}{\underline{p}} + \left(\frac{\bar{p}\bar{h}}{\underline{r}}\right)^2 \frac{m}{\underline{p}}$. □

Now, we prove Theorem 4.1.

Proof of Theorem 4.1. We define a Lyapunov function

$$V_t(e_t) = \mathbf{e}_t^T \mathbf{P}_t^{-1} \mathbf{e}_t. \quad (60)$$

By using (29), we write

$$\frac{1}{\bar{p}} \|\mathbf{e}_t\|^2 \leq V_t(\mathbf{e}_t) \leq \frac{1}{\underline{p}} \|\mathbf{e}_t\|^2. \quad (61)$$

By using (26), we have

$$\begin{aligned} V_{t+1}(\mathbf{e}_{t+1}) &= \mathbf{e}_t^T (\mathbf{I} - \mathbf{K}_t \mathbf{H}_t)^T \mathbf{P}_t^{-1} (\mathbf{I} - \mathbf{K}_t \mathbf{H}_t) \mathbf{e}_t \\ &\quad + \mathbf{r}_t^T \mathbf{P}_{t+1} [2(\mathbf{I} - \mathbf{K}_t \mathbf{H}_t) \mathbf{e}_t + \mathbf{r}_t] \\ &\quad + 2\mathbf{s}_t^T \mathbf{P}_{t+1} [(\mathbf{I} - \mathbf{K}_t \mathbf{H}_t) \mathbf{e}_t + \mathbf{r}_t] + \mathbf{s}_t^T \mathbf{P}_{t+1}^{-1} \mathbf{s}_t. \end{aligned}$$

Taking the conditional expectation of both sides and using Lemma 4.3, 4.4 and 4.5, we write

$$E[V_{t+1}(\mathbf{e}_{t+1})|\mathbf{e}_t] \leq (1 - \alpha)V_t(\mathbf{e}_t) + \kappa_{\text{nonl}}\|\mathbf{e}_t\|^3 + \kappa_{\text{noise}}\delta. \quad (62)$$

Say $\epsilon = \min\left(\epsilon_\chi, \frac{\alpha}{2\bar{p}\kappa_{\text{nonl}}}\right)$. For $\|\mathbf{e}_t\| \leq \epsilon$

$$\kappa_{\text{nonl}}\|\mathbf{e}_t\|\|\mathbf{e}_t\|^2 \leq \frac{\alpha}{2\bar{p}}\|\mathbf{e}_t\|^2 \leq \frac{\alpha}{2}V_t(\mathbf{e}_t). \quad (63)$$

Then for $\|\mathbf{e}_t\| \leq \epsilon$, we write

$$E[V_{t+1}(\mathbf{e}_{t+1})|\mathbf{e}_t] - V_t(\mathbf{e}_t) \leq -\frac{\alpha}{2}V_t(\mathbf{e}_t) + \kappa_{\text{noise}}\delta. \quad (64)$$

In order to ensure that $E[V_{t+1}(\mathbf{e}_{t+1})|\mathbf{e}_t] - V_t(\mathbf{e}_t) \leq 0$, we choose

$$\delta = \frac{\alpha\tilde{\epsilon}^2}{2\bar{p}\kappa_{\text{noise}}} \quad (65)$$

with some $\tilde{\epsilon} < \epsilon$. By [35, Lemma 2.1] and equations in (64)-(65), $\|\mathbf{e}_t\|$ is exponentially bounded in the mean square. Thus, the DEKF learning algorithm asymptotically converges to the local optimum with probability one. \square

Remark 4.3. *We emphasize that in Theorem 4.1, we do not represent the effect of grouping the weights as an additional non-linearity as in the IEKF learning algorithm. Instead, by realizing the similarity between the Kalman gain formulations of GEKF and DEKF, we represent the effect of decoupling as a perturbation in the state covariance matrix update in (21)-(22). Then by considering the effect of this perturbation as additional process noise in (31), we derive sufficient conditions for the stability of the DEKF used in the online training of the considered LSTM model in (1)-(7).*

We point out that the presented theoretical guarantees in this section are valid also for GEKF, where $g = 1$, $\mathbf{D}_1 = \mathbf{I}$ in (22), and $\tilde{\lambda}_t = 0$ for $t \geq 0$ in (31). We additionally note that the presented theoretical guarantees for both GEKF and DEKF depend on the lower bound of their noise terms (see Lemma 4.3), where these noise terms are selected by the user as the hyper-parameters. Therefore, we say that if our noise term selection in DEKF satisfies (31) without diverging the

training, the DEKF learning algorithm learns the LSTM parameters with similar theoretical properties of GEKF. In the next section, we verify this result by using the well-known parameter selection approaches for DEKF in the literature [15, 27, 39].

5. Numerical Evaluation

In the preceding section, we conclude that if our hyper-parameter selection satisfies (31) without diverging the training, DEKF learns the LSTM parameters with similar convergence properties of GEKF. In this section, we demonstrate the implications of our theoretical conclusion with numerical simulations. To this end, we use DEKF with the well-known hyper parameter selection approaches in the literature [31, 32, 34]. The main approach in these studies is as follows:

- We note that the artificial measurement noise term \mathbf{R}_t acts as a smoother in the Kalman gain matrix formulation in (19). Therefore, it is selected such that $\mathbf{R}_t \gg \{\mathbf{P}_t\}_{t \geq 1}$ to satisfy the incremental-step assumption in the RTRL algorithm [21].
- The artificial process noise term \mathbf{Q}_t is demonstrated to enhance the speed of convergence in the neural network training [34]. It is usually selected a small value as such $q_t \in [10^{-6}, 10^{-3}]$.

In the simulations, we use two different datasets, i.e., the kinematic dataset [40] and Alcoa stock price dataset [41]. In DEKF and IEKF, we follow the most widely used grouping approach in the literature, i.e., grouping by node, where $g = (4n_s + 1)$ [27, 31, 32, 34]. We note that this variant of DEKF is called *the node decoupled EKF* in the literature, and it has quadratic computational complexity in the parameter size under the condition of $n_s = O(n_i)$ [32]. In the following, we compare four different algorithms: GEKF, IEKF, the node decoupled EKF with the parameter selection strategy described in the previous paragraph (DEKF), and the stochastic gradient descent algorithm (SGD). We note that we use SGD as the baseline algorithm to compare the second-order EKF-based training methods.

5.1. Kinematic Dataset

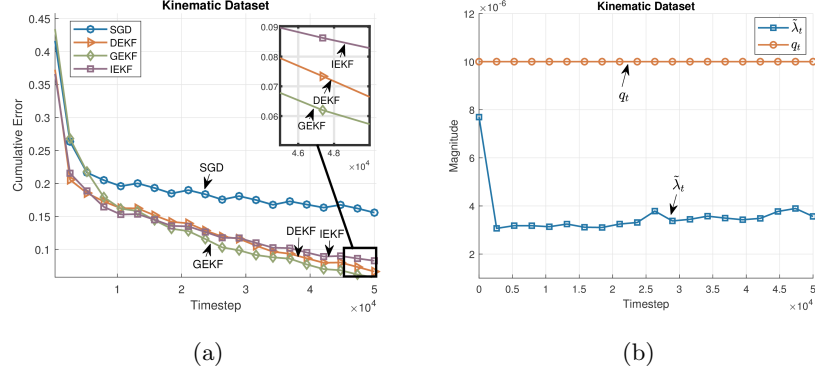


Figure 3: (a) Sequential prediction performances of the algorithms for the kinematic dataset. (b) Comparison between the process noise level q_t and $\tilde{\lambda}_t$ -defined in (32)- in DEKF.

In the first experiment, we use the kinematic dataset [40], i.e., a simulation of eight-link all-revolute robotic arm. Here, our aim is to predict the distance of the end-effector from its target. As the desired data \mathbf{d}_t , we use the distance value at time t , i.e., $n_d = 1$. As the input data \mathbf{x}_t , we use the last previous four distance values and a bias term, i.e., $n_i = 5$. In our LSTM model, we use 4-dimensional hidden state vectors, i.e., $n_s = 4$, to get small training error with a relatively lower run-time. Note that this experiment can be alternatively considered as an LSTM-based system identification, where we only observe the distance values to identify the dynamics of the considered robotic arm system.

To be able to compare the algorithms based on our theoretical work, we use the same hyper-parameters and same weight initialization in each algorithm. We draw the initial values for all the weights from a Gaussian distribution with zero mean and standard deviation of 0.5. In the EKF-based training algorithms, we initialize the initial state covariance matrix as $\mathbf{P}_0 = 0.1\mathbf{I}$. As the covariance matrix of the artificial noise terms, we use $\mathbf{R}_t = 10\mathbf{I}$ and $\mathbf{Q}_t = 10^{-5}\mathbf{I}$ for $t \geq 0$. In SGD, we use the best learning rate, i.e., $\mu = 0.05$, in terms of the performance at the end of the training. We run the algorithms with a training

length of $T = 5 \times 10^4$. We repeat the simulations 25 times and provide the mean performances in Fig. 3.

As we observe in Fig. 3a, the EKF-based methods provide comparable performance while they outperform the SGD algorithm. Furthermore, in Fig. 3a and 3b, we observe that the widely used hyper-parameter selection approach with the selected values satisfies (31) without diverging the training. This result, based on our theoretical work, explains the comparable performance of DEKF and GEKF in the considered online LSTM-based learning problem, which is also in parallel with the empirical results in the literature [31, 32, 34].

5.2. Alcoa Stock Price Dataset

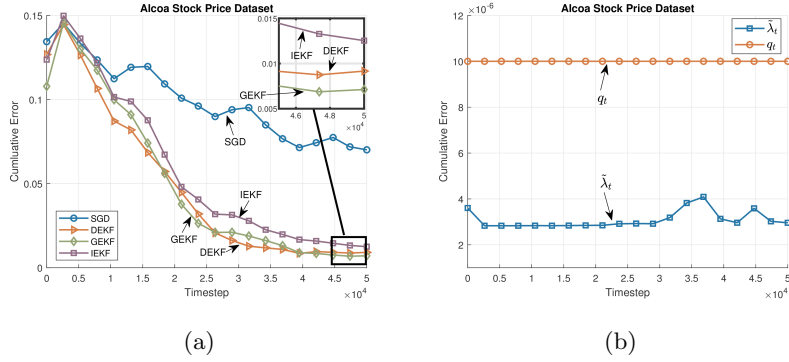


Figure 4: (a) Sequential prediction performances of the algorithms for the Alcoa stock price dataset. (b) Comparison between the process noise q_t and $\tilde{\lambda}_t$ -defined in (32)- in DEKF.

In the second experiment, we use the Alcoa stock price dataset [41], which contains the daily stock prices of Alcoa Corporation. Here, our goal is to predict the lowest price of the stock in the next day by examining the past prices. As the desired data \mathbf{d}_t , we use the lowest value of the stock price in day t , i.e., $n_d = 1$. As the input data \mathbf{x}_t , we use the highest, lowest, opening and closing stock prices of day $t - 1$ with a bias term, i.e., $n_i = 5$. In our LSTM model, we use 4-dimensional hidden state vectors, i.e., $n_s = 4$, to get small training error with a relatively lower run-time.

To compare the algorithms, we use the same hyper-parameters as in the first experiment, i.e., $\mathbf{P}_0 = 0.1\mathbf{I}$, $\mathbf{R}_t = 10\mathbf{I}$ and $\mathbf{Q}_t = 10^{-5}\mathbf{I}$ for $t \geq 0$ in the EKF-based methods, and $\mu = 0.05$ in SGD. We draw the initial values for all the weights from a Gaussian distribution with zero mean and standard deviation of 0.5, and use the same initialization in each algorithm. We run the algorithms with a training length of $T = 5 \times 10^4$, repeat the simulations 25 times, and plot the mean performances in Fig. 4.

In Fig. 4a, we observe that GEKF and DEKF provide comparable performance, where they are slightly better than IEKF. Furthermore, as expected, all the EKF-based algorithms significantly outperform SGD. Similar to the previous experiment, in Fig. 4b, we observe that our parameter selection satisfy (31) without divergence. This result explains the comparable performance of GEKF and DEKF in this considered problem as well.

6. Concluding Remarks

We studied the stability and the convergence properties of the DEKF within the LSTM-based online learning framework. By realizing the similarity between the Kalman gain formulations of GEKF and DEKF, we represented the effect of decoupling as a perturbation in the state covariance matrix update of the GEKF learning algorithm. Then by considering the effect of this perturbation as additional process noise, we derived sufficient conditions for the stability of the DEKF used in the online training of the considered LSTM model. We additionally demonstrated that if the perturbations introduced due to decoupling stay bounded, DEKF learns the LSTM parameters with similar theoretical properties of the GEKF learning algorithm by reducing its computational requirement to quadratic computational complexity in the parameter size. We verified our theoretical results with several numerical simulations and compared DEKF with the conventional LSTM training methods. In the experimentation, we observed that the well-known hyper-parameter selection approaches used for DEKF in the literature [31, 32, 34] provide comparable performance with

GEKF while satisfying our mathematically proven conditions. Therefore, we additionally provided theoretically founded experimental results, which can be used as a benchmark in future LSTM-based online learning studies.

Appendix A. Jacobian Calculation

For this section, we introduce three new notations: Given vector \mathbf{u} , $\text{diag}(\mathbf{u})$ is the diagonal matrix constructed from the entries of \mathbf{u} . \mathbf{u}^2 stands for the element-wise square, i.e., $\mathbf{u}^2 = \mathbf{u} \odot \mathbf{u}$. Given matrix $\mathbf{A} = [\mathbf{a}_1, \mathbf{a}_2, \dots, \mathbf{a}_n]$ and vector \mathbf{u} , $\mathbf{A} \odot \mathbf{u} = [\mathbf{a}_1 \odot \mathbf{u}, \mathbf{a}_2 \odot \mathbf{u}, \dots, \mathbf{a}_n \odot \mathbf{u}]$.

In this section, we derive the Jacobian matrix \mathbf{H}_t given in (12). We note that $\mathbf{H}_{i,t}$ matrices given in (17) are the columns of \mathbf{H}_t corresponding to θ_i . Therefore, the following equations are general in the sense that they can be used for the GEKF, the IEKF and the DEKF.

To derive the Jacobian matrix \mathbf{H}_t , we use the real time recurrent learning (RTRL) algorithm [21]. To this end, let us define $\mathbf{C}_t, \mathbf{D}_t \in \mathbb{R}^{n_s \times n_\theta}$ such that $\mathbf{C}_t = (\partial \mathbf{y}_t / \partial \boldsymbol{\theta})$ and $\mathbf{D}_t = (\partial \mathbf{c}_t / \partial \boldsymbol{\theta})$. By (1)-(6), we can write

$$\mathbf{H}_t = \frac{\partial \hat{\mathbf{d}}_t}{\partial \boldsymbol{\theta}} = \frac{\partial \hat{\mathbf{d}}_t}{\partial \mathbf{y}_t} \frac{\partial \mathbf{y}_t}{\partial \boldsymbol{\theta}} \quad (\text{A.1})$$

$$= \frac{\partial \hat{\mathbf{d}}_t}{\partial \mathbf{y}_t} \mathbf{C}_t \quad (\text{A.2})$$

where

$$\mathbf{C}_t = \frac{\partial \mathbf{y}_t}{\partial \boldsymbol{\theta}} = \frac{\partial \mathbf{y}_t}{\partial \mathbf{y}_{t-1}} \frac{\partial \mathbf{y}_{t-1}}{\partial \boldsymbol{\theta}} + \frac{\partial \mathbf{y}_t}{\partial \mathbf{c}_t} \frac{\partial \mathbf{c}_t}{\partial \boldsymbol{\theta}} + \frac{\partial \mathbf{y}_t}{\partial \boldsymbol{\theta}_t} \frac{\partial \boldsymbol{\theta}_t}{\partial \boldsymbol{\theta}} \quad (\text{A.3})$$

$$= \frac{\partial \mathbf{y}_t}{\partial \mathbf{y}_{t-1}} \mathbf{C}_{t-1} + \frac{\partial \mathbf{y}_t}{\partial \mathbf{c}_t} \mathbf{D}_t + \frac{\partial \mathbf{y}_t}{\partial \boldsymbol{\theta}_t} \quad (\text{A.4})$$

and

$$\frac{\partial \mathbf{y}_t}{\partial \mathbf{y}_{t-1}} = \frac{\partial \mathbf{y}_t}{\partial \mathbf{o}_t} \frac{\partial \mathbf{o}_t}{\partial \mathbf{y}_{t-1}} + \frac{\partial \mathbf{y}_t}{\partial \mathbf{c}_t} \frac{\partial \mathbf{c}_t}{\partial \mathbf{y}_{t-1}} \quad (\text{A.5})$$

$$\frac{\partial \mathbf{y}_t}{\partial \boldsymbol{\theta}_t} = \frac{\partial \mathbf{y}_t}{\partial \mathbf{o}_t} \frac{\partial \mathbf{o}_t}{\partial \boldsymbol{\theta}_t} + \frac{\partial \mathbf{y}_t}{\partial \mathbf{c}_t} \frac{\partial \mathbf{c}_t}{\partial \boldsymbol{\theta}_t}. \quad (\text{A.6})$$

Similarly, we can write

$$\mathbf{D}_t = \frac{\partial \mathbf{c}_t}{\partial \boldsymbol{\theta}} = \frac{\partial \mathbf{c}_t}{\partial \mathbf{c}_{t-1}} \frac{\partial \mathbf{c}_{t-1}}{\partial \boldsymbol{\theta}} + \frac{\partial \mathbf{c}_t}{\partial \mathbf{y}_{t-1}} \frac{\partial \mathbf{y}_{t-1}}{\partial \boldsymbol{\theta}} + \frac{\partial \mathbf{c}_t}{\partial \boldsymbol{\theta}_t} \frac{\partial \boldsymbol{\theta}_t}{\partial \boldsymbol{\theta}} \quad (\text{A.7})$$

$$= \frac{\partial \mathbf{c}_t}{\partial \mathbf{c}_{t-1}} \mathbf{D}_{t-1} + \frac{\partial \mathbf{c}_t}{\partial \mathbf{y}_{t-1}} \mathbf{C}_{t-1} + \frac{\partial \mathbf{c}_t}{\partial \boldsymbol{\theta}_t} \quad (\text{A.8})$$

where

$$\frac{\partial \mathbf{c}_t}{\partial \mathbf{y}_{t-1}} = \frac{\partial \mathbf{c}_t}{\partial \mathbf{i}_t} \frac{\partial \mathbf{i}_t}{\partial \mathbf{y}_{t-1}} + \frac{\partial \mathbf{c}_t}{\partial \mathbf{z}_t} \frac{\partial \mathbf{z}_t}{\partial \mathbf{y}_{t-1}} + \frac{\partial \mathbf{c}_t}{\partial \mathbf{f}_t} \frac{\partial \mathbf{f}_t}{\partial \mathbf{y}_{t-1}} \quad (\text{A.9})$$

$$\frac{\partial \mathbf{c}_t}{\partial \boldsymbol{\theta}_t} = \frac{\partial \mathbf{c}_t}{\partial \mathbf{i}_t} \frac{\partial \mathbf{i}_t}{\partial \boldsymbol{\theta}_t} + \frac{\partial \mathbf{c}_t}{\partial \mathbf{z}_t} \frac{\partial \mathbf{z}_t}{\partial \boldsymbol{\theta}_t} + \frac{\partial \mathbf{c}_t}{\partial \mathbf{f}_t} \frac{\partial \mathbf{f}_t}{\partial \boldsymbol{\theta}_t}. \quad (\text{A.10})$$

We note that in (A.4) and (A.8), we use $(\partial \boldsymbol{\theta}_t / \partial \boldsymbol{\theta}) = \mathbf{I}$ due to (8).

By using (4), one can easily derive $(\partial \mathbf{c}_t / \partial \mathbf{i}_t) = \text{diag}(\mathbf{z}_t)$, $(\partial \mathbf{c}_t / \partial \mathbf{z}_t) = \text{diag}(\mathbf{i}_t)$, $(\partial \mathbf{c}_t / \partial \mathbf{f}_t) = \text{diag}(\mathbf{c}_{t-1})$, $(\partial \mathbf{c}_t / \partial \mathbf{c}_{t-1}) = \text{diag}(\mathbf{f}_t)$. Similarly, by (6), $(\partial \mathbf{y}_t / \partial \mathbf{o}_t) = \text{diag}(\tanh(\mathbf{c}_t))$ and $(\partial \mathbf{y}_t / \partial \mathbf{c}_t) = \text{diag}(\mathbf{o}_t \odot (1 - \tanh(\mathbf{c}_t)^2))$.

To derive $(\partial \mathbf{o}_t / \partial \mathbf{y}_{t-1})$, let us use $\mathbf{W}_t^{(o)} \in \mathbb{R}^{n_s \times (n_s + n_i)}$ to denote the weight matrix used in the output gate at time t and say

$$\mathbf{W}_t^{(o)} = [\mathbf{W}_t^{(o,1)}, \mathbf{W}_t^{(o,2)}] \quad (\text{A.11})$$

where $\mathbf{W}_t^{(o,1)} \in \mathbb{R}^{n_s \times n_i}$ and $\mathbf{W}_t^{(o,2)} \in \mathbb{R}^{n_s \times n_s}$ such that

$$\mathbf{o}_t = \sigma(\mathbf{W}_t^{(o,1)} \mathbf{x}_t + \mathbf{W}_t^{(o,2)} \mathbf{y}_{t-1}). \quad (\text{A.12})$$

By applying chain rule, one can derive

$$\frac{\partial \mathbf{o}_t}{\partial \mathbf{y}_{t-1}} = \mathbf{W}_t^{(o,2)} \odot \mathbf{o}_t \odot (1 - \mathbf{o}_t). \quad (\text{A.13})$$

By using the same notation in (A.11) for the weight matrices of the other gates and by applying the chain rule, one can show that

$$\frac{\partial \mathbf{i}_t}{\partial \mathbf{y}_{t-1}} = \mathbf{W}_t^{(i,2)} \odot \mathbf{i}_t \odot (1 - \mathbf{i}_t) \quad (\text{A.14})$$

$$\frac{\partial \mathbf{f}_t}{\partial \mathbf{y}_{t-1}} = \mathbf{W}_t^{(f,2)} \odot \mathbf{f}_t \odot (1 - \mathbf{f}_t) \quad (\text{A.15})$$

$$\frac{\partial \mathbf{i}_t}{\partial \mathbf{y}_{t-1}} = \mathbf{W}_t^{(z,2)} \odot (1 - \mathbf{z}_t^2) \quad (\text{A.16})$$

$$\frac{\partial \hat{\mathbf{d}}_t}{\partial \mathbf{y}_t} = \mathbf{W}_t^{(d,2)} \odot \hat{\mathbf{d}}_t \odot (1 - \hat{\mathbf{d}}_t). \quad (\text{A.17})$$

For $(\partial \mathbf{o}_t / \partial \boldsymbol{\theta}_t)$, we first note that the derivative of the \mathbf{o}_t with respect to the entries of $\boldsymbol{\theta}_t$ corresponding to $\mathbf{W}^{(i)}$, $\mathbf{W}^{(f)}$, $\mathbf{W}^{(z)}$, and $\mathbf{W}^{(d)}$ and is 0. Then let us use $\boldsymbol{\theta}_t^{(o)}$ to refer the entries of the $\boldsymbol{\theta}_t$ corresponding to $\mathbf{W}_t^{(o)}$. By using (A.12), one can show that

$$\frac{\partial \mathbf{o}_t}{\partial \boldsymbol{\theta}_t^{(o)}} = \mathbf{L}_t \odot \mathbf{o}_t \odot (\mathbf{1} - \mathbf{o}_t) \quad (\text{A.18})$$

where $\mathbf{L}_t \in \mathbb{R}^{n_s \times n_s (n_i + n_s)}$ such that

$$\mathbf{L}_t = \begin{bmatrix} \mathbf{x}_t^T & \mathbf{y}_{t-1}^T & \mathbf{0} & \mathbf{0} & \dots & \mathbf{0} & \mathbf{0} \\ \mathbf{0} & \mathbf{0} & \mathbf{x}_t^T & \mathbf{y}_{t-1}^T & \dots & \mathbf{0} & \mathbf{0} \\ \vdots & \vdots & \vdots & \vdots & \ddots & \vdots & \vdots \\ \mathbf{0} & \mathbf{0} & \mathbf{0} & \mathbf{0} & \dots & \mathbf{x}_t^T & \mathbf{y}_{t-1}^T \end{bmatrix}. \quad (\text{A.19})$$

By using a similar notation used in (A.18), one can write that

$$\frac{\partial \mathbf{i}_t}{\partial \boldsymbol{\theta}_t^{(i)}} = \mathbf{L}_t \odot \mathbf{o}_t \odot (\mathbf{1} - \mathbf{o}_t) \quad (\text{A.20})$$

$$\frac{\partial \mathbf{f}_t}{\partial \boldsymbol{\theta}_t^{(f)}} = \mathbf{L}_t \odot \mathbf{o}_t \odot (\mathbf{1} - \mathbf{f}_t) \quad (\text{A.21})$$

$$\frac{\partial \mathbf{z}_t}{\partial \boldsymbol{\theta}_t^{(z)}} = \mathbf{L}_t \odot (\mathbf{1} - \mathbf{z}_t^2). \quad (\text{A.22})$$

For $(\partial \hat{\mathbf{d}}_t / \partial \boldsymbol{\theta}_t)$, we can write,

$$\frac{\partial \hat{\mathbf{d}}_t}{\partial \boldsymbol{\theta}_t} = \frac{\partial \hat{\mathbf{d}}_t}{\partial \mathbf{y}_t} \frac{\partial \mathbf{y}_t}{\partial \boldsymbol{\theta}_t} + [\mathbf{0}, \frac{\partial \hat{\mathbf{d}}_t}{\partial \boldsymbol{\theta}_t^{(d)}}] \quad (\text{A.23})$$

where $(\partial \hat{\mathbf{d}}_t / \partial \boldsymbol{\theta}_t^{(d)})$ can be derived as in (A.20)-(A.22) but by using \mathbf{y}_t in (A.19) instead of \mathbf{y}_{t-1} .

By assuming $n_d \leq n_s$, the most expensive operations in this algorithm is (A.4), particularly $(\partial \mathbf{y}_t / \partial \mathbf{y}_{t-1}) \mathbf{C}_{t-1}$. Therefore, the complexity of the algorithm is $O(n_s^3(n_s + n_i)) \approx O(n_\theta^2)$.

References

- [1] N. Cesa-Bianchi, G. Lugosi, Prediction, Learning, and Games, Cambridge University Press, New York, NY, USA, 2006 (2006).

- [2] V. G. Vovk, Aggregating strategies, in: Proceedings of the Third Annual Workshop on Computational Learning Theory, COLT '90, Morgan Kaufmann Publishers Inc., San Francisco, CA, USA, 1990, pp. 371–386 (1990).
- [3] E. E. Kuruolu, Nonlinear least lp-norm filters for nonlinear autoregressive-stable processes, Digital Signal Processing 12 (1) (2002) 119 – 142 (2002). doi:<https://doi.org/10.1006/dspr.2001.0416>.
URL <http://www.sciencedirect.com/science/article/pii/S1051200401904166>
- [4] M. B. Malik, M. Salman, State-space least mean square, Digital Signal Processing 18 (3) (2008) 334 – 345 (2008). doi:<https://doi.org/10.1016/j.dsp.2007.05.003>.
URL <http://www.sciencedirect.com/science/article/pii/S1051200407000899>
- [5] A. C. Singer, G. W. Wornell, A. V. Oppenheim, Nonlinear autoregressive modeling and estimation in the presence of noise, Digital Signal Processing 4 (4) (1994) 207 – 221 (1994). doi:<https://doi.org/10.1006/dspr.1994.1021>.
URL <http://www.sciencedirect.com/science/article/pii/S1051200484710219>
- [6] N. D. Vanli, M. A. Donmez, S. S. Kozat, Robust least squares methods under bounded data uncertainties, Digital Signal Processing 36 (2015) 82 – 92 (2015). doi:<https://doi.org/10.1016/j.dsp.2014.10.004>.
URL <http://www.sciencedirect.com/science/article/pii/S1051200414003133>
- [7] J. Y. Goulermas, P. Liatsis, X. Zeng, P. Cook, Density-driven generalized regression neural networks (dd-grnn) for function approximation, IEEE Transactions on Neural Networks 18 (6) (2007) 1683–1696 (Nov 2007). doi:[10.1109/TNN.2007.902730](https://doi.org/10.1109/TNN.2007.902730).

- [8] M. N. Seyman, N. Tapnar, Channel estimation based on neural network in space time block coded mimoofdm system, Digital Signal Processing 23 (1) (2013) 275 – 280 (2013). doi:<https://doi.org/10.1016/j.dsp.2012.08.003>.
URL <http://www.sciencedirect.com/science/article/pii/S1051200412001728>
- [9] G. Dede, M. H. Sazl, Speech recognition with artificial neural networks, Digital Signal Processing 20 (3) (2010) 763 – 768 (2010). doi:<https://doi.org/10.1016/j.dsp.2009.10.004>.
URL <http://www.sciencedirect.com/science/article/pii/S1051200409001821>
- [10] F. Stulp, O. Sigaud, Many regression algorithms, one unified model: A review, Neural Networks 69 (2015) 60 – 79 (2015). doi:<https://doi.org/10.1016/j.neunet.2015.05.005>.
URL <http://www.sciencedirect.com/science/article/pii/S0893608015001185>
- [11] D. F. Specht, A general regression neural network, IEEE Transactions on Neural Networks 2 (6) (1991) 568–576 (Nov 1991). doi:[10.1109/72.97934](https://doi.org/10.1109/72.97934).
- [12] K. Kanjamapornkul, R. Pink, S. Chunithipaisan, E. Barto, Support spinor machine, Digital Signal Processing 70 (2017) 59 – 72 (2017). doi:<https://doi.org/10.1016/j.dsp.2017.07.023>.
URL <http://www.sciencedirect.com/science/article/pii/S1051200417301732>
- [13] D. Kari, A. H. Mirza, F. Khan, H. Ozkan, S. S. Kozat, Boosted adaptive filters, Digital Signal Processing 81 (2018) 61 – 78 (2018). doi:<https://doi.org/10.1016/j.dsp.2018.07.012>.
URL <http://www.sciencedirect.com/science/article/pii/S1051200418305335>

- [14] Y. Engel, S. Mannor, R. Meir, The kernel recursive least-squares algorithm, *IEEE Transactions on Signal Processing* 52 (8) (2004) 2275–2285 (Aug 2004). doi:10.1109/TSP.2004.830985.
- [15] S. Haykin, *Neural Networks: A Comprehensive Foundation*, 2nd Edition, Prentice Hall PTR, Upper Saddle River, NJ, USA, 1998 (1998).
- [16] Long-term time series prediction with the narx network: An empirical evaluation, *Neurocomputing* 71 (16) (2008) 3335 – 3343, advances in Neural Information Processing (ICONIP 2006) / Brazilian Symposium on Neural Networks (SBRN 2006) (2008).
- [17] N. D. Vanli, M. O. Sayin, I. Delibalta, S. S. Kozat, Sequential nonlinear learning for distributed multiagent systems via extreme learning machines, *IEEE Transactions on Neural Networks and Learning Systems* 28 (3) (2017) 546–558 (March 2017). doi:10.1109/TNNLS.2016.2536649.
- [18] J. Schmidhuber, Deep learning in neural networks: An overview, *CoRR* abs/1404.7828 (2014). arXiv:1404.7828.
URL <http://arxiv.org/abs/1404.7828>
- [19] U. Shaham, A. Cloninger, R. R. Coifman, Provable approximation properties for deep neural networks, *Applied and Computational Harmonic Analysis* 44 (3) (2018) 537 – 557 (2018). doi:<https://doi.org/10.1016/j.acha.2016.04.003>.
URL <http://www.sciencedirect.com/science/article/pii/S1063520316300033>
- [20] M. Hermans, B. Schrauwen, Training and analysing deep recurrent neural networks, in: C. J. C. Burges, L. Bottou, M. Welling, Z. Ghahramani, K. Q. Weinberger (Eds.), *Advances in Neural Information Processing Systems* 26, Curran Associates, Inc., 2013, pp. 190–198 (2013).
- [21] R. J. Williams, D. Zipser, A learning algorithm for continually running fully recurrent neural networks, *Neural Computation* 1 (1989) 270–280 (1989).

- [22] Y. Bengio, P. Y. Simard, P. Frasconi, Learning long-term dependencies with gradient descent is difficult, *IEEE transactions on neural networks* 5 2 (1994) 157–66 (1994).
- [23] S. Hochreiter, J. Schmidhuber, Long short-term memory, *Neural Computation* 9 (1997) 1735–1780 (1997).
- [24] P. J. Werbos, Backpropagation through time: what it does and how to do it, *Proceedings of the IEEE* 78 (10) (1990) 1550–1560 (Oct 1990). doi:10.1109/5.58337.
- [25] T. Ergen, S. S. Kozat, Efficient online learning algorithms based on lstm neural networks, *IEEE Transactions on Neural Networks and Learning Systems* 29 (8) (2018) 3772–3783 (Aug 2018). doi:10.1109/TNNLS.2017.2741598.
- [26] J. Martens, I. Sutskever, Learning recurrent neural networks with hessian-free optimization, in: *Proceedings of the 28th International Conference on International Conference on Machine Learning, ICML’11*, Omnipress, USA, 2011, pp. 1033–1040 (2011).
URL <http://dl.acm.org/citation.cfm?id=3104482.3104612>
- [27] J. Antonio Prez-Ortiz, F. Gers, D. Eck, J. Schmidhuber, Kalman filters improve lstm network performance in problems unsolvable by traditional recurrent nets, *Neural networks : the official journal of the International Neural Network Society* 16 (2003) 241–50 (04 2003). doi:10.1016/S0893-6080(02)00219-8.
- [28] N. Laptev, J. Yosinski, E. L. Li, S. Smyl, Time-series extreme event forecasting with neural networks at uber, 2017 (2017).
- [29] J. Press, Lstm online training and prediction: Non-stationary real time data stream forecasting (10 2018).
- [30] S. Singhal, L. Wu, Training multilayer perceptrons with the extended kalman algorithm (1989) 133–140 (01 1989).

- [31] S. Haykin, Kalman filtering and neural networks, 2001 (2001).
- [32] G. V. Puskorius, L. A. Feldkamp, Neurocontrol of nonlinear dynamical systems with kalman filter trained recurrent networks, *IEEE Transactions on Neural Networks* 5 (2) (1994) 279–297 (March 1994). doi:10.1109/72.279191.
- [33] R. J. Williams, Some observations on the use of the extended kalman filter as a recurrent network learning algorithm, Tech. rep. (1992).
- [34] G. V. Puskorius, L. A. Feldkamp, Decoupled extended kalman filter training of feedforward layered networks, in: *IJCNN-91-Seattle International Joint Conference on Neural Networks*, Vol. i, 1991, pp. 771–777 vol.1 (July 1991). doi:10.1109/IJCNN.1991.155276.
- [35] K. Reif, S. Gunther, E. Yaz, R. Unbehauen, Stochastic stability of the discrete-time extended kalman filter, *IEEE Transactions on Automatic Control* 44 (4) (1999) 714–728 (April 1999). doi:10.1109/9.754809.
- [36] G. V. Puskorius, L. A. Feldkamp, Extensions and enhancements of decoupled extended kalman filter training, in: *Proceedings of International Conference on Neural Networks (ICNN'97)*, Vol. 3, 1997, pp. 1879–1883 vol.3 (June 1997). doi:10.1109/ICNN.1997.614185.
- [37] S. Shah, F. Palmieri, Meka-a fast, local algorithm for training feedforward neural networks, in: *1990 IJCNN International Joint Conference on Neural Networks*, 1990, pp. 41–46 vol.3 (June 1990). doi:10.1109/IJCNN.1990.137822.
- [38] W. A. Sutherland, *Introduction to Metric and Topological Spaces*, Oxford University Press, U.S.A. (2 ed.), 2009 (2009).
- [39] G. Puskorius, L. Feldkamp, Decoupled extended kalman filter training of feedforward layered networks, 1991, pp. 771 – 777 vol.1 (08 1991). doi:10.1109/IJCNN.1991.155276.

- [40] C. E. R. et al., Delve data sets, <http://www.cs.toronto.edu/~delve/data/datasets.html>, accessed: 2019-06-21.
- [41] A. Inc., Common stock, <http://finance.yahoo.com/quote/AA?ltr=1>, accessed: 2019-06-21.